

**Weierstraß-Institut**  
**für Angewandte Analysis und Stochastik**  
**Leibniz-Institut im Forschungsverbund Berlin e. V.**

Preprint

ISSN 2198-5855

**Adjustable pulse compression scheme for generation of  
few-cycle pulses in the mid-infrared**

Ayhan Demircan<sup>1</sup>, Shalva Amiranashvili<sup>2</sup>, Carsten Brée<sup>2</sup>,

Uwe Morgner<sup>1</sup>, Günter Steinmeyer<sup>3</sup>

submitted: Februar 12, 2014

<sup>1</sup> Leibniz Universität Hannover  
Welfengarten 1  
30167 Hannover  
Germany  
E-Mail: demircan@iqo.uni-hannover.de  
morgner@iqo.uni-hannover.de

<sup>2</sup> Weierstraß-Institut  
Mohrenstraße 39  
10117 Berlin  
Germany  
E-Mail: Shalva.Amiranashvili@wias-berlin.de  
Carsten.Bree@wias-berlin.de

<sup>3</sup> Max-Born-Institute  
Max-Born-Str. 2a  
12489 Berlin  
Germany  
E-Mail: steinmey@mbi-berlin.de

No. 1926  
Berlin 2014



---

2010 *Physics and Astronomy Classification Scheme*. 42.65.Re, 42.65.Ky, 42.65.Tg, 42.81.Dp.

*Key words and phrases*. Pulse compression, Ultrashort pulses, Optical event horizons, Nonlinear Schrödinger equation.

Sh.A. gratefully acknowledges support by the DFG Research Center MATHEON (project D 14), and A.D. by the DFG.

Edited by  
Weierstraß-Institut für Angewandte Analysis und Stochastik (WIAS)  
Leibniz-Institut im Forschungsverbund Berlin e. V.  
Mohrenstraße 39  
10117 Berlin  
Germany

Fax: +49 30 20372-303  
E-Mail: [preprint@wias-berlin.de](mailto:preprint@wias-berlin.de)  
World Wide Web: <http://www.wias-berlin.de/>

## Abstract

An novel adjustable adiabatic soliton compression scheme is presented, enabling a coherent pulse source with pedestal-free few-cycle pulses in the infrared or mid-infrared regime. This scheme relies on interaction of a dispersive wave and a soliton copropagating at nearly identical group velocities in a fiber with enhanced infrared transmission. The compression is achieved directly in one stage, without necessity of an external compensation scheme. Numerical simulations are employed to demonstrate this scheme for silica and fluoride fibers, indicating ultimate limitations as well as the possibility of compression down to the single-cycle regime. Such output pulses appear ideally suited as seed sources for parametric amplification schemes in the mid-infrared.

The generation of pulses in the single-cycle regime has advanced in a variety of wavelength regimes. Methods include pulse compression of Ti:sapphire oscillator and amplifier pulses [1, 2, 3], coherent synthesis of compressed pulses [4, 5], optical rectification [6], attosecond pulse generation via high-harmonic generation [7] as well as optical parametric amplification [8]. Despite the impressive spread of wavelengths, ranging from the vacuum ultraviolet into the terahertz regime, there still are apparent gaps, e.g., in the mid-infrared from 2–10  $\mu\text{m}$ . While there exist nonlinear optical crystals that offer favorable phase matching properties and efficiency in this region [9], it is often the unavailability of convenient broadband coherent seed sources that limits parametric amplification schemes in the mid infrared.

In this paper we demonstrate a tunable compression scheme for pedestal-free few-cycle pulses applicable in a wide spectral range. Our scheme is based on enhanced cross-phase modulation (XPM) [10, 11] mediated by an optical event horizon [12, 13]. This principle has already been demonstrated for an efficient all-optical control of pulses [14, 15] and for broadband supercontinuum generation with superior coherence [16]. However, the dispersion properties of the fiber dictate limitations for optimization of the pulse manipulation. Here we show how one can overcome these limitations and further exploit the mechanism for direct soliton self-compression. The compression is inherently provided by a collision process and is achieved directly in one stage, without necessity of an external compensation scheme. In particular, we demonstrate the possibility of compression down to single-cycle duration in fused silica fibers. This mechanism even appears improved in fluoride fibers with larger compression factor and high efficacy in the mid-infrared. This scheme represents an alternative route to facilitate the generation of short coherent pulses in the infrared and mid-infrared in combination with direct tunability of the pulse width, as demonstrated exemplarily for fused silica and ZBLAN fluoride fibers.

For our investigations we performed numerical simulations of the nonlinear pulse propagation directly for the electric field using the unidirectional propagation equation for the analytical signal  $\mathcal{E}(z, t) = 2 \sum_{\omega>0} E_{\omega} e^{-i\omega t}$  [17]

$$i\partial_z \mathcal{E} + \hat{\beta} \mathcal{E} + \frac{n_2}{c} \partial_t (f_K |\mathcal{E}|^2 \mathcal{E} + f_R \mathcal{E} \hat{h} |\mathcal{E}|^2)_+ = 0, \quad (1)$$

where  $f_K$  and  $f_R = 1 - f_K$  describe relative contributions of the Kerr and Raman effect,

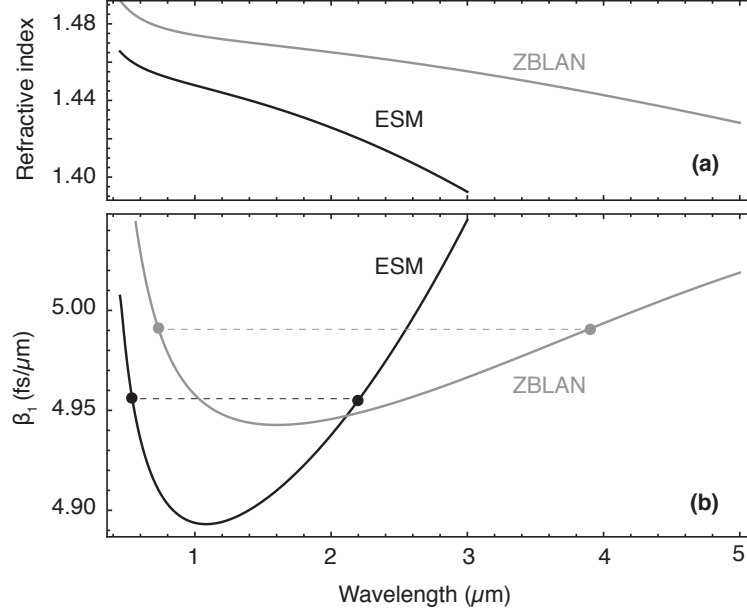


Figure 1: (a) Refractive index of a microstructured fiber (ESM fused silica) and a ZBLAN fluorid fiber. (b) Corresponding relative group delay  $\beta_1$  with adequate resonant frequency combinations (see text). The ZBLAN fiber allows center frequencies for fundamental solitons at far separation from the zero dispersion wavelength.

respectively, and  $\hat{h}$  denotes convolution with the Raman response function

$$\hat{h}|\mathcal{E}(z, t)|^2 = \int_0^\infty h(t')|\mathcal{E}(z, t - t')|^2 dt',$$

where

$$h(t') = \frac{\tau_1^2 + \tau_2^2}{\tau_1 \tau_2^2} e^{-t'/\tau_2} \sin(t'/\tau_1).$$

We adopt values  $\tau_1 = 9$  fs,  $\tau_2 = 134$  fs, and  $f_R = 0.1929$  for fluoride fiber, and  $\tau_1 = 12.5$  fs,  $\tau_2 = 32$  fs, and  $f_R = 0.18$  for fused silica [18].

The main precondition of our scheme is the establishment of an optical event horizon by an effective refractive index barrier between two pulses copropagating at nearly identical group velocities [12, 13]. The refractive index barrier is created by a soliton via cross-phase modulation and acts on a dispersive wave. This condition can always be fulfilled for fibers with at least one zero dispersion wavelength (ZDW), allowing adequate frequency combinations for a dispersive wave and a fundamental soliton in the normal and anomalous dispersion regime, respectively. Figure 1(a) displays the refractive index of a microstructured endlessly single mode (ESM) fiber [19] and that of a ZBLAN fiber [20]. The ESM fiber, which consists of fused silica, becomes highly absorbing above  $2.5\mu\text{m}$ , limiting the range of fundamental soliton propagation on the long wavelength side. Fluoride glasses as ZBLAN, in contrast, exhibit high transmission well into the mid infrared, which enables multi-octave separated frequency combinations traveling at equal group velocity [Fig. 1(b)].

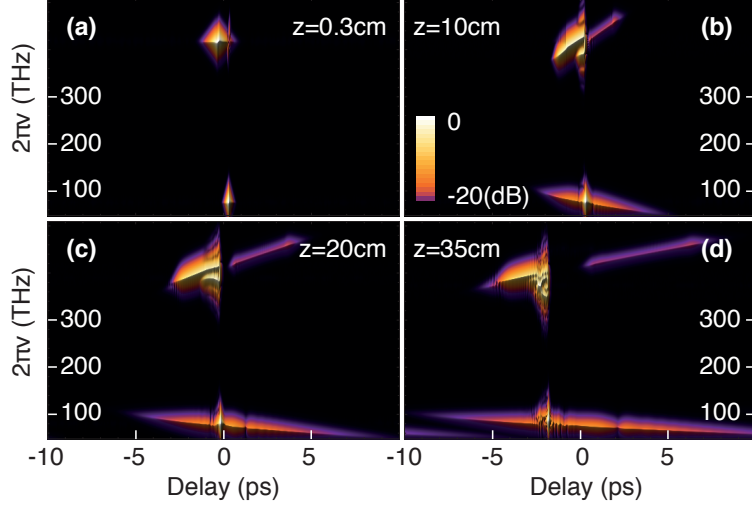


Figure 2: XFROG spectrogram at (a) 0.2 cm, (b) 10 cm, (c) 20 cm, and (d) 30 cm for the collision of a DW at the refractive index barrier created at the leading edge of a FS. The optical event horizon appears as a vertical line moving with the center frequency shift of the soliton.

For efficient manipulation in any of the discussed schemes [16, 21, 22], it is necessary to launch the soliton into a spectral range with a strong  $\beta_3$ . Small soliton frequency shifts then already lead to strong adiabatic pulse reshaping due to the steep slope of  $\beta_2(\omega)$ . If the soliton is shifted into a region with decreased dispersion, this slope will lead to adiabatic soliton compression. The mechanism is widely similar to soliton compression in dispersion decreasing fibers (DDF), where a decrease of  $\beta_2(z)$  stems from a prefabricated fiber diameter variation along  $z$  [23]. Other than in the DDF system, we adjust the effective dispersion for the soliton by the frequency shift, such that the center frequencies of initial and compressed soliton differ from each other. For dispersion profiles as shown in Fig. 1, soliton compression is accomplished by a collision process between a dispersive wave (DW) and the soliton. This collision induces a blue shift of the soliton center frequency. Such collision processes are depicted in Fig. 2 as XFROG spectrograms with evolving propagation along  $z$ . For proof-of-principle considerations, let us first neglect the Raman effect. We choose  $A_0 = 0.0226$  and  $t_0 = 44.36$  fs for the fundamental soliton (FS) and  $A_0 = 0.017$  and  $t_0 = 100$  fs for the DW. The initial center frequencies correspond to the frequency combination  $\omega_0 = 2.6177$  and  $0.4709$  rad/fs (4000nm) for the DW and the FS, respectively. The FS is injected with a time delay of 450 fs into the fiber relative to the DW. The spectrograms are shown in the moving frame of an undisturbed soliton, with zero delay located halfway between the two pulses.

Already after 0.2 cm of copropagation, the establishment of an optical event horizon can be observed. After 10 cm [Fig. 2(b)], the DW appears dispersively broadened in time, resulting in an increased interaction with the soliton. A small part of the DW is able to pass the soliton-induced barrier, but the main part is delayed. In the moving frame of the soliton, this process appears as an effective reflection at the group-velocity horizon [12] and shows up as newly generated spectral content at longer wavelength. Simultaneously, the soliton peak intensity strongly increases, and the pulse width decreases. The soliton also starts to radiate energy into the anomalous dispersion regime. This transfer relies on the fact that the selected compression example does not

correspond to an ideal adiabatic change of the soliton. As the center frequency is slightly shifted to shorter wavelengths, the refractive index barrier is also shifted accordingly. With further propagation this mechanism appears enhanced, with spectral broadening of the soliton [Fig. 2(c)] accompanied by strong compression. At the end of the fiber [Fig. 2(d)], nearly the entire energy of the DW has been transferred to negative delays beyond the horizon. This effective reflection in the frame of the soliton has also been termed the “optical push broom effect”, which was first observed in a fiber Bragg grating [24].

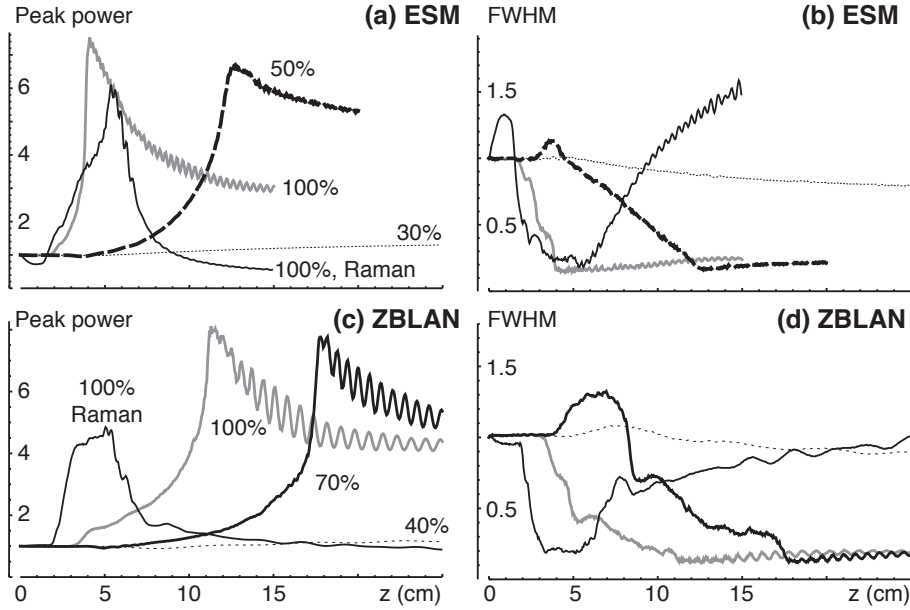


Figure 3: (a) The induced evolution of the relative peak power of the soliton for different peak powers of the DW in the ESM fiber. The ratio between the peak powers of the DW and the soliton are  $P_{DW}/P_S = 0.3, 0.5, 1$ . (b) Corresponding evolution of the relative soliton pulse width. (c) Relative soliton peak power evolution in the ZBLAN fiber for  $P_{DW}/P_S = 0.4, 0.7, 1$ . (d) Corresponding relative soliton pulse width evolution. Calculations with the impact of the Raman effect are performed for  $P_S = P_{DW}$  (thin black lines).

In our compression scheme, the frequency shift of the soliton is induced by the dispersive wave, which enables control of this process by varying pulse parameters or by shaping the DW. In this way, the soliton output pulse width can be adjusted at fixed FS input parameters. For example, the peak intensity of the dispersive wave can be used as an efficient and easy-to-adjust control parameter. Other possible control parameters are the pulse width and the initial delay between FS and DW.

Figure 3(a,b) depicts the evolution of the relative peak power and relative pulse width of the soliton along  $z$  for different DW intensities in the ESM fiber. In this example, the best compression performance is achieved for a peak intensity ratio  $P_{DW}/P_S = 0.5$  (thick black line). Similar results are achieved with inclusion of the Raman effect (thin black line), yet require a more careful adaption of the frequency combination. Stronger intensities of the DW may lead to an increased penetration of the barrier. In turn, this leakage process eventually leads to degraded compression behavior (grey line). This deterioration can easily be avoided by adjusting the initial time

delay between the two pulses. However, there is another limiting factor. We observe that despite of stronger shifts of the soliton center frequency, the pulses cannot further be compressed. This shortcoming appears due to a growing overlap of the soliton spectrum with the normal dispersion regime. Depending on the amount of this detrimental overlap, the compressed few-cycle soliton may even be destroyed when energy is transferred from the soliton into the continuum. In this case, the soliton falls back into a solution with a broader pulse duration. This effect becomes more important for initial frequency combinations with frequencies closer to the ZDW. Overlap with the normal dispersion regime therefore appears as the main limitation for efficient compression in fused silica fibers. Better performance is only possible for media with extremely wide transparency region, allowing fundamental soliton propagation at wavelengths widely separated from the ZDW, as demonstrated here exemplarily for a ZBLAN fluoride fiber [Fig. 3(c),(d)]. We expect that the same mechanism can also be applied for selenide or telluride fibers with low-loss transmission reaching into the far-infrared.

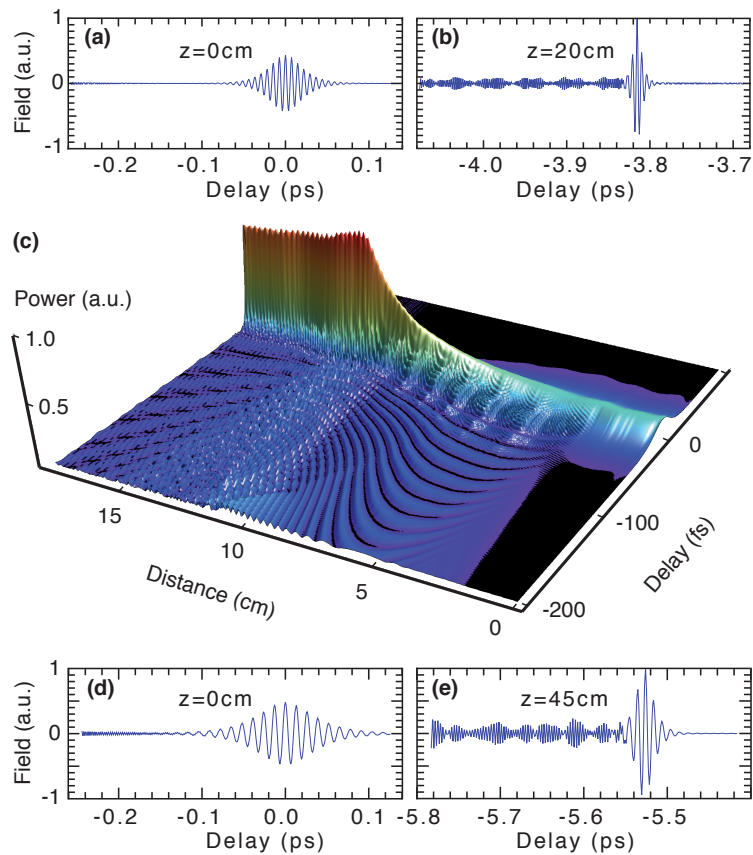


Figure 4: Adiabatic pulse compression of a soliton close to the single-cycle regime. (a) Electric field of the initial soliton, (b) calculated output electric field, (c) time domain evolution of the intensities in the co-moving frame of the soliton for the scenario shown in Fig. 3(a, thick black line). (d) Initial electric field and (e) output field for the optimal compression factor in the transmission region of the ZBLAN fiber 800 – 4500nm for the scenario in Fig. 3(c, thick black line).

Figure 4(c) demonstrates the compression of the FS along the propagation distance  $z$  for optimum conditions in the ESM fiber [Fig. 3(a,b) thick black line]. The evolution is shown in the

moving frame of the soliton. The input soliton exhibits a duration of five cycles and is compressed to nearly single-cycle duration when shifted to an output wavelength  $\lambda_c = 3760\text{nm}$ . The corresponding compression factor  $\tau_c = t_0/t_{\text{out}}$  is about five, but for a short  $z$ -interval at about  $z = 13\text{ cm}$ , it exceeds the factor of six, i.e., we observe a duration in the sub-cycle regime. The electric field for the initial soliton and the output solitons are shown in Figs. 4(a) and (b), respectively. The output pulses correspond to fundamental solitons and are therefore free of any pedestal. The substructures belong to the dispersive waves, with wavelengths in the short-wavelength regime that can easily be filtered out. Qualitatively the same behavior is observed for the ZBLAN fiber. To provide a direct comparison, we used the same cycle number for the input pulse as for the ESM fiber. For the optimum scenario in Fig. 3(c, thick black line), the electric fields of the input and the output soliton are depicted in Fig. 4(d) and (e), respectively. As the limitation for the soliton compression appears reduced for the ZBLAN fiber, higher compression factors are possible.

In order to investigate the viability of our approach as a source of few-cycle and single-cycle pulses in the mid-infrared, we performed numerous simulations in the transmission region of the ZBLAN fiber. In the entire wavelength region  $2.5\text{--}5\ \mu\text{m}$ , we observe essentially identical compression behavior, with output solitons in the sub-2-cycle regime. In contrast, the compression possibility in the ESM is less efficient, although the possibility for generating ultrashort pulses into the few-cycle regimes range and below is given, see Figs. 3(a,b).

Our simulations impressively show how the concept of two pulses interacting in the group-velocity horizon can be suitably tailored to adiabatically compress solitons in the infrared or mid-infrared in a ESM or ZBLAN fiber, respectively. Starting with a fixed many-cycle pulse, our scheme allows a controlled compression close to the single-cycle limit. Resulting output pulses may serve as an ideal seed for broadband parametric schemes in the mid-infrared. The compression is realized directly in one stage and can be controlled in manifold ways by a dispersive wave. This method opens a completely new perspective for a relatively straightforward and un-critical pulse synthesis scheme, which is applicable for different media and wavelengths. Such sources could close an important gap in the single-cycle regime, enabling unprecedented temporal resolution in the molecular finger-printing regime.

## References

- [1] A. L. Cavalieri, E. Goulielmakis, B. Horvath, W. Helml, M. Schultze, M. Fieß, V. Pervak, L. Veisz, V. S. Yakovlev, M. Uiberacker, A. Apolonski, F. Krausz, and R. Kienberger, *New J. Phys.* **9**, 242 (2007).
- [2] G. Steinmeyer and G. Stibenz, *Appl. Phys. B* **82**, 175–182 (2006).
- [3] E. Matsubara, K. Yamane, T. Sekikawa, and M. Yamashita, *J. Opt. Soc. Am. B* **24**, 985–989 (2007).
- [4] A. Wirth, M. T. Hassan, I. Grguraš, J. Gagnon, A. Moulet, T. T. Luu, S. Pabst, R. Santra, Z. A. Alahmed, A. M. Azzeer, V. S. Yakovlev, V. Pervak, F. Krausz, E. Goulielmakis, *Science* **334**, 195–200 (2011).

- [5] J. A. Cox, W. P. Putnam, A. Sell, A. Leitenstorfer, and F. X. Kärtner, *Opt. Lett.* **37**, 3579–3581 (2012).
- [6] D. You, D. R. Dykaar, R. R. Jones, and P. H. Bucksbaum, *Opt. Lett.* **18**, 290–292 (1993).
- [7] K. Zhao, Q. Zhang, M. Chini, Y. Wu, X. Wang, and Z. Chang, *Opt. Lett.* **37**, 3891–3893 (2012).
- [8] C. Manzoni, S.-W. Huang, G. Cirimi, P. Farinello, J. Moses, F. X. Kärtner, and G. Cerullo, *Opt. Lett.* **37**, 1880–1882 (2012).
- [9] D. E. Zelmon, E. A. Hanning, and P. G. Schunemann, *J. Opt. Soc. Am. B* **18**, 1307–1310 (2001).
- [10] D. V. Skryabin and A. V. Yulin, *Phys. Rev. E* **72**, 016619 (2005)
- [11] D. V. Skryabin and A. V. Gorbach, *Rev. Mod. Phys.* **82**, 1287–1299 (2010).
- [12] T. G. Philbin, C. Kuklewicz, S. Robertson, S. Hill, F. König, and U. Leonhardt, *Science* **319**, 1367-1370 (2008).
- [13] D. Faccio, *Cont. Phys.* **1**,1-16 (2012).
- [14] A. Demircan, Sh. Amiranashvili, and G. Steinmeyer, *Phys. Rev. Lett.* **106**, 163901 (2011).
- [15] R. Driben, F. Mitschke, and N. Zhavoronkov, *Opt. Exp.* **18**, 25993 (2010).
- [16] A. Demircan, Sh. Amiranashvili, C. Brée, and G. Steinmeyer, *Phys. Rev. Lett.* **110**, 233901 (2013).
- [17] Sh. Amiranashvili and A. Demircan, *Phys. Rev. A* **82**, 013812 (2010).
- [18] G. Agrawal, *Nonlinear Fiber Optics.* (Academic Press, San Diego, 2001).
- [19] J.M. Stone and J.C. Knight, *Opt. Express* **16**, 2670 (2008).
- [20] C. Agger, C. Petersen, S. Dupont, H. Steffensen, J. K. Lyngso, C. L. Thomsen, J. Thogersen, S. R. Keiding, and O. Bang, *J. Opt. Soc. Am. B* **21**, 635 (2012).
- [21] A. Demircan, Sh. Amiranashvili, C. Brée, Ch. Mahnke, F. Mitschke, and G. Steinmeyer, *Sci. Rep.* **2**, 850 (2012).
- [22] R. Driben and I. Babushkin, *Opt. Lett.* **37**, 5157 (2012).
- [23] S.V. Chernikov, D.J. Richardson, D.N. Payne, and E.M. Dianov, *Opt. Lett.* **18**, 476–478 (1993).
- [24] C.M. De Sterke, *Opt. Lett.* **17**, 914 (1992).